Optoacoustic detection of thermal lesions

Michel G. Arsenault[1], Michael C. Kolios[2] and William M. Whelan[1,3]

[1]Department of Physics, University of Prince Edward Island, Charlottetown (Canada)
[2]Department of Physics, Ryerson University, Toronto (Canada)
[3]Department of Biomedical Sciences, Atlantic Veterinary College, Charlottetown (Canada)

ABSTRACT

Minimally invasive thermal therapy is being investigated as an alternative cancer treatment. It involves heating tissues to greater than 55°C over a period of a few minutes, which results in tissue coagulation. Optoacoustic (OA) imaging is a new imaging technique that involves exposing tissues to pulsed light and detecting the acoustic waves that are generated. In this study, adult bovine liver tissue samples were heated using continuous wave laser energy for various times, then scanned using an optoacoustic imaging system. Large optoacoustic signal variability was observed in the native tissue prior to heating. OA signal amplitude increased with maximum tissue temperature achieved, characterized by a correlation coefficient of 0.63. In this study we show that there are detectable changes in optoacoustic signal strength that arise from tissue coagulation, which demonstrates the potential of optoacoustic technology for the monitoring of thermal therapy delivery.

Keywords: optoacoustic, imaging, thermal lesions, liver

1. INTRODUCTION

Optoacoustic detection combines the penetration depth, high resolution and rapid data acquisition of ultrasound with the rich tissue contrast possible with optical interrogation.[1] Central to this technique is the optoacoustic effect, a process by which tissue is irradiated with nanosecond laser pulses yielding a local temperature rise followed by thermal expansion, thereby producing acoustic waves.[1] The amplitude and shape of the pressure transients created in tissues depend on the light fluence (i.e. intensity) and the contrast between the optical and thermo-mechanical properties of the target absorber and the surrounding media. Typically, enhanced optical absorption by blood leads to stronger pressure signals compared to background signals from tissues.[2]

Minimally invasive thermal therapy has been explored as a means of treating small solid tumours.[3,4] It involves heating the target tissue to temperatures between 55°C and 95°C for several minutes which results in coagulative necrosis. This is differentiated from *hyperthermia*, which involves lower temperature (40°C to 45°C) and longer**,** multiple applications (several tens of minutes) and has been used in conjunction with muti-fractionated radiation or chemotherapy. Thermal therapy is typically delivered as a single-fraction, stand-alone therapy. It can potentially achieve highly conformal 3D coagulation volumes, exhibits sharp demarcation between treated and spared tissues, allows for selective sparing of adjacent normal structures via localized cooling, and tissue effects can be observed (and thus potentially controlled and optimized) in real time.[5] The high temperatures induced during thermal therapy cause dynamic changes in the optical, mechanical and thermal properties of tissues and cause vascular shutdown. The temperature dependence, magnitude, and extent of these changes are not well known, but the presence of these time-varying tissue properties makes the pre-treatment prediction (i.e. treatment planning) of the resulting coagulation volume very difficult. In addition, if tissue temperatures exceed 100°C, tissue charring may occur, which should be avoided. Hence treatment guidance is needed to ensure complete tumour coverage without damaging the surrounding healthy tissue. Various minimally or non-invasive methods of guiding and monitoring thermal therapy have been investigated, including fluoroptic temperature sensors[6], magnetic resonance temperature imaging[7], the use of radiance/fluence probes[8], and ultrasound imaging. [9]

In this study we obtain optoacoustic signals from unheated and heated bovine liver *ex vivo* and investigate the influence of tissue coagulation on optoacoustic measurements.

Photons Plus Ultrasound: Imaging and Sensing 2009, edited by Alexander A. Oraevsky, Lihong V. Wang,
Proc. of SPIE Vol. 7177, 71771V · © 2009 SPIE · CCC code: 1605-7422/09/$18 · doi: 10.1117/12.810913

2. MATERIALS & METHODS

2.1 Thermal lesions

Frozen adult bovine liver was rapidly brought to room temperature by thawing in water. Thermal lesions were generated on the surface of the tissue using a multimode optical fiber with 1000µm core diameter and numerical aperture 0.37 (ThorLabs, Newton, NJ, USA), coupled to a Diomed 60, 810nm diode laser (Diomed, Cambridge, UK). For each experiment, 6 thermal lesions were created using a constant power of 1.3-1.6W for 1 to 6 minutes, increasing by 1 minute intervals, with the optic fiber at a distance of 13mm to the surface of the tissue. The tissue was allowed to cool to room temperature after each lesion was generated.

A calibrated thermal camera (FLIR ThermaCAM SC2000) with a 34/80 close-up lens (FLIR Systems, Burlington, On, Canada) was used to collect thermal data. Data was collected using ThermaCAM Researcher Pro 2.8 software (FLIR Systems, Burlington, On, Canada) at a rate of one frame per second during heating as well as for 5 seconds prior to start of heating and for 15 seconds after the laser was turned off. These temperature maps provided information about the surface tissue temperature during heating. The experimental protocol was repeated for 7 liver samples.

2.2 Optoacoustic detection

A small amount of ultrasound coupling gel (Parker Laboratories, Fairfield, NJ, USA) was placed on the liver surface and the tissue was vacuum-sealed in a polyethylene bag. The tissue sample was attached to a vertical holder and fixed in the waterbath of an optoacoustic imaging system (Imagio, Seno Medical, San Antonio, TX, USA). The imaging system consisted of an 8 element annular array transducer (4 MHz central frequency) and an Nd:YAG pumped and Ti:Sapphire laser. A bifurcated optical fiber bundle delivered pulsed optical energy at 775 nm or 1064 nm with 70 mJ energy, 6 ns duration, and 10 Hz repetition rate (Figure 1). The nominal illumination beam diameter on the liver surface was 9 mm. The transducer array / fiber assembly raster scanned across the front of the tissue sample at 0.2 mm steps. Optoacoustic data was acquired from 1.5 mm by 1.5 mm regions of interest (ROI) at the center of thermal lesion and in the native tissue adjacent to the lesion (Figure 2a). Hence, 64 individual A-lines, representing an average of 8 measurements each were acquired within each ROI. Signals were amplified and averages were stored.

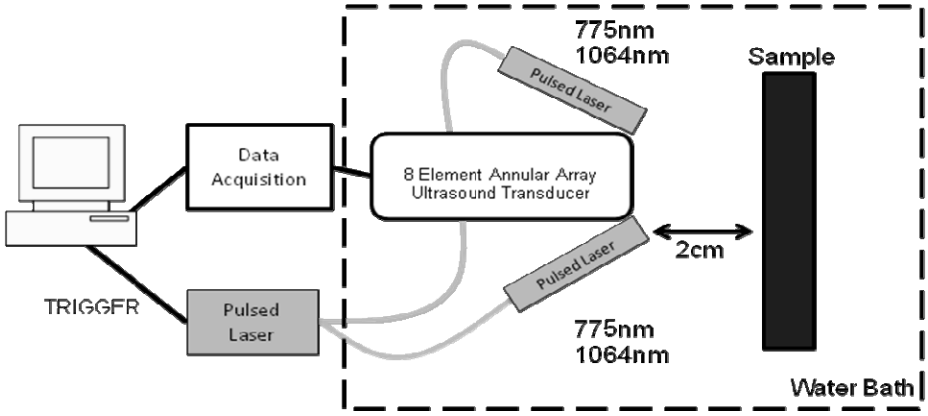

Figure 1. Schematic representation of the optoacoustic imaging system

2.3 Data analysis

All thermal and optoacoustic data were exported to Matlab for analysis. For the maximum temperature profiles, the last frame of the thermal data before laser was turned off was used and analyzed. An average maximum temperature was calculated over the ROI surrounding the maximum temperature for each lesion. Maximum temperature was assumed to occur at the center of the thermal lesion and the area selected for average dose calculation was confirmed to be approximately at geometrical center of lesions based on the thermal data (Figure 2b).

Optoacoustic signals for 775 nm illuminations were analyzed. The Hilbert transform was applied to all optoacoustic A-lines and the data presented as arbitrary signal strength. The peak amplitude of the Hilbert transform, from the front surface of tissue samples, was used for subsequent analysis to compare optoacoustic signals from native and coagulated regions.

3. RESULTS

Six thermal lesions created on the surface of *ex vivo* bovine liver, for exposure durations of 1 to 6 minutes, are shown in Figure 2a (one of the seven tissue experiments). Significant variability was observed in visible coagulation both between lesions (Figure 2a) and between experiments for the same heating protocols (data not shown). The increased extent of visible coagulation did not always correlate well with increased heating times. Variations in the tissue optical properties across the sample may account for some of this variability. Surface thermal images of each lesion were acquired separately and are shown in a composite image (see Figure 2b). The averaged maximum temperature achieved over the ROI for each lesion is shown. It is worth noting that the standard deviations are small compared to the absolute temperature. Interestingly, the maximum temperature for the 5 minute exposure time was greater than for the 6 minute exposure time. This may be due to variation in the optical absorption coefficient across the liver surface.

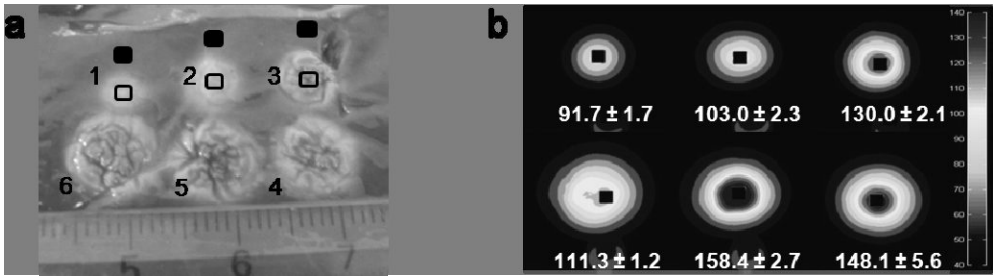

Figure 2. **(a)** Representative photograph of lesions. Areas of optoacoustic scans for lesions 1-3 are indicated, similar ROIs were also used for lesions 4-6. Empty boxes are on lesion, full boxes are on native tissue. Numbers adjacent to lesions indicate time in minutes laser was on. **(b)** Composite image of maximum temperature profiles obtained from experiment shown in (a). Boxes are of same size as ROIs scanned with the optoacoustic imager and encompass values used to calculate average maximum temperatures. Maximum temperature (°C) ± 1 standard deviation are indicated under each profile. Signal artifacts at bottom of images are the optical fiber.

Lesions were allowed to cool to room temperature before the OA data was acquired to avoid temperature effects from confounding the analysis. Representative A-lines (n=64), for a 775 nm illumination, obtained from a 1.5 mm by 1.5 mm ROI in native liver are shown in Figure 3. The corresponding 64 Hilbert transforms are also shown. The front surface of the liver sample corresponds to ~ 14 μs. In Figure 3, the peak amplitude of the Hilbert transform increases by 136 % from the native to the coagulated state.

Optoacoustic signal strengths, as measured by the peak amplitude of the Hilbert transform, for native and coagulated *ex vivo* bovine liver tissue are shown in Figures 4a and 4b, respectively. Inter- and intra-sample variability in optoacoustic signals from native tissues is observed. This is likely due to natural variation in the optical absorption coefficient of liver. For coagulated liver, the optoacoustic signals increase with heating time, but the variability over each scanned area appeared to increase with heating times, with the most variability observed at the center of charred tissue (Figure 4b). A general trend of increasing signal strength with maximum temperature achieved can be observed for most of the 7 experiments.

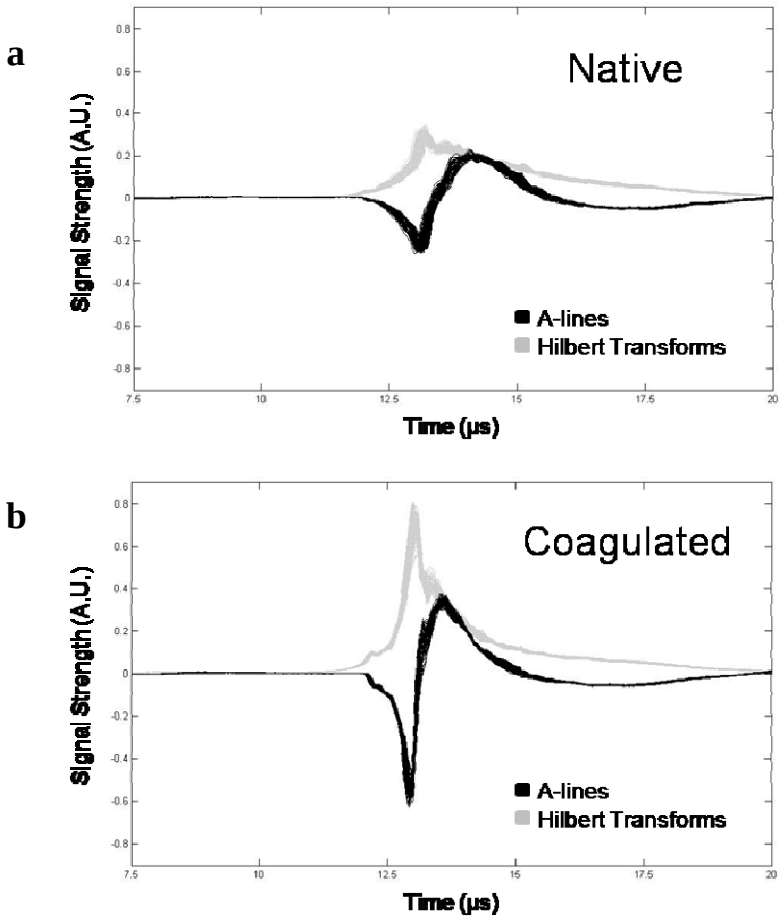

Figure 3. Representative optoacoustic A-lines (n=64 superimposed) and corresponding Hilbert transforms from **(a)** native and **(b)** adjacent coagulated liver regions. The illumination wavelength was 775 nm.

Due to the variability observed in the optoacoustic signals from the native bovine liver tissue, we performed a pair-wise subtraction to obtain the difference in signal strengths on and off lesion as a function of laser heating time. This provided a measure of absolute signal increase as a function of laser heating time for each tissue sample (Figure 4c). The percentage change in optoacoustic signal for all lesions except those where charring was observed are plotted against maximum temperature achieved (Figure 5). A Pearson's correlation coefficient of r = 0.63 is obtained, which represents a weak positive correlation.

Optoacoustic signal generation is proportional to the product of the optical absorption coefficient, the local optical fluence, and the thermo-acoustic efficiency (called the Gruneisen parameter). The surface illumination used in the present study provides for a consistent optical fluence between experiments such that the observed differences in signal strength are likely due to changes in the optical absorption and/or thermo-acoustic efficiency. Ritz et al[10] reported a moderate increase in the optical absorption coefficient in porcine liver *ex vivo* after coagulation between 400 and 900 nm and a reduction from 900 nm to 1350 nm. This suggests that 775 nm illumination may be preferred over 1064 nm for optoacoustic detection of tissue coagulation. Soroushian et al.[11] reported a 65 % increase in the Gruneissen parameter after coagualtion in tissue mimicking albumen phantoms. Hence, the positive correlation between optoacoustic signal strength and maximum temperature achieved observed in this study is consistent with increased tissue optical absorption and thermo-acoustic efficiency.

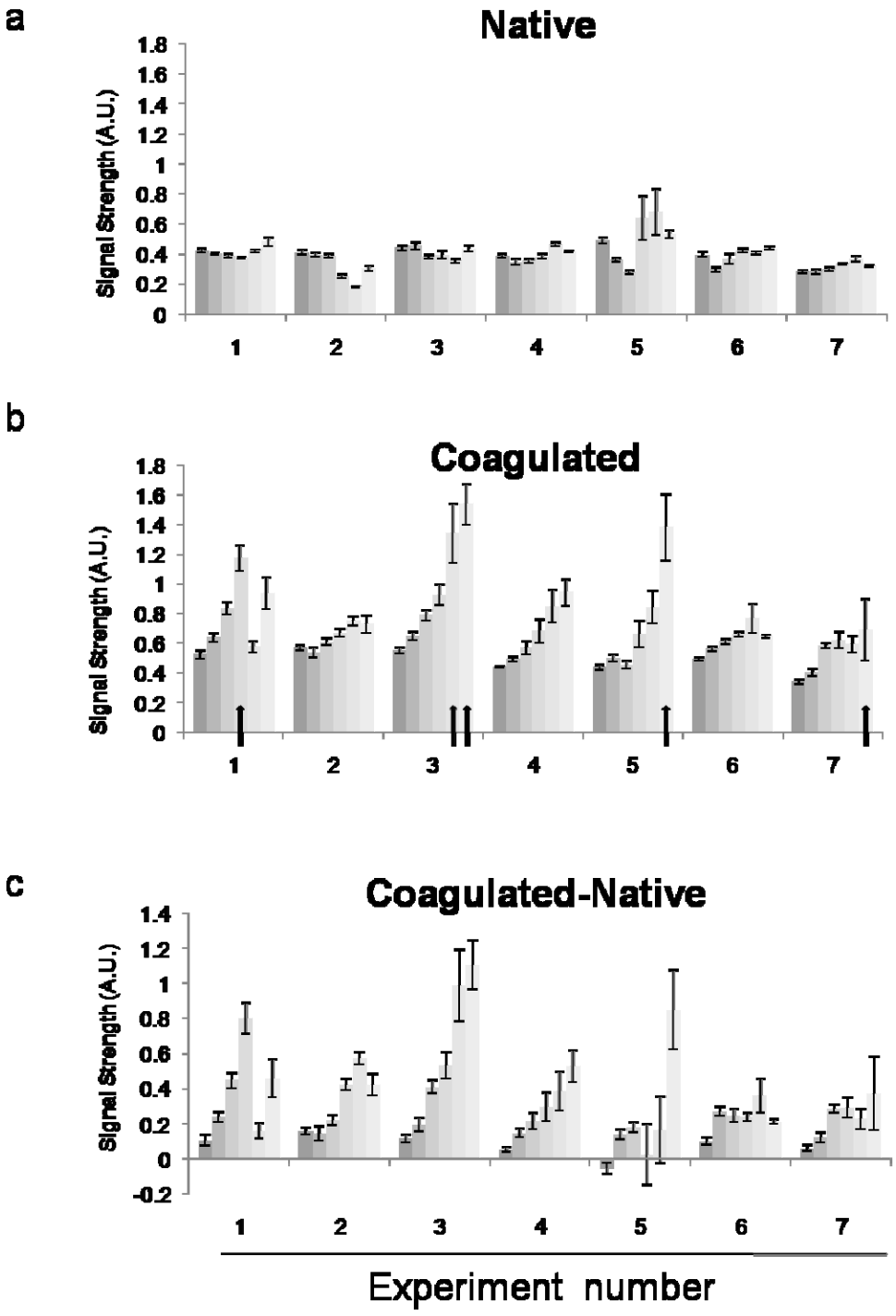

Figure 4. **(a)** Average of maximum optoacoustic values at front surface of native tissue obtained from all 7 experiments. **(b)** Average of maximum optoacoustic values at front surface of coagulated tissue obtained for all 7 experiments. Arrows indicate lesions where tissue charring occurred. **(c)** Average values of pair-wise increase of maximum optoacoustic values at front surface of coagulated over native tissue values obtained for all 7 experiments. (For each of the 7 experiments data is presented as 6 individual bars representing areas 1 to 6 from left to right. Average signal strength ± 1 standard deviation are presented for all data).

In evaluating the results, it should be noted that thermal camera temperature measurements require knowledge of the tissue emissivity. The emissivity of native and coagulated bovine liver is not well known. Preliminary measurements as part of this study yielded values of 0.95 and 0.75 for native and coagulated states respectively. However, the analysis software does not allow for a changing emissivity. Hence, a coagulated emissivity value was used when converting the transient infrared data to temperature which will result in a slight overestimation of temperature.

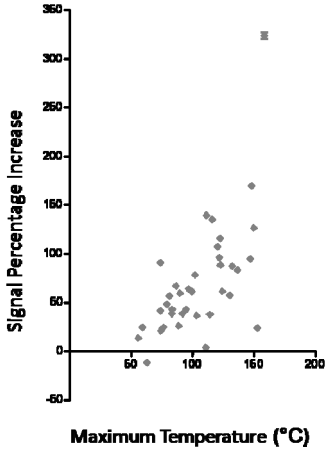

Figure 5. Scatter plot of pair-wise percent increase in optoacoustic signal versus maximum temperature reached during heating. Note that optoacoustic signals were collected after tissue was cooled. Pearson's correlation coefficient r = 0.63 for n=37 data points.

4. CONCLUSIONS

In this study we found large variability in optoacoustic signals from native *ex vivo* bovine liver tissue. Through our experimentation, we also found that calculating energy deposition is insufficient to predict thermal lesion formation as different final temperatures were achieved using the same laser heating protocol. This is of great clinical importance for minimally invasive thermal therapy and demonstrates why close monitoring of therapy delivery on an individual basis, in real time, is essential. Our results demonstrate that optoacoustic signal increases with maximum temperature achieved, such that optoacoustics may be suitable candidate for monitoring of thermal therapy delivery and merits further investigation.

5. ACKNOWLEDGEMENTS

The authors would like to thank Mike Harris, Don Herzog and Matthew Fronheiser from Seno Medical Instruments for their technical advice, and Michelle MacPhee and Kris Lund from the Department of Physics at the University of Prince Edward Island for their helpful discussions.

REFERENCES

1. Oraevsky, A.A. & Karabuto, A.A. (eds.) Optoacoustic tomography. (CRC, New York; 2003).

2. Ku, G., Wang, X., Xie, X., Stoica, G. & Wang, L.V. "Imaging of tumor angiogenesis in rat brains in vivo by photoacoustic tomography". *Applied Optics* **44**, 770-775 (2005).

3. Diederich CJ (2005) "Thermal ablation and high-temperature thermal therapy: overview of technology and clinical implementation" *International Journal of Hyperthermia*, 21(8):745-753.

4. Nau WH, Diederich CJ, Ross AB, Butts K, Rieke V, Bouley DM, Gill H, Daniel B and Sommer G (2005), "MRI-guided interstitial ultrasound thermal therapy of the prostate: A feasibility study in the canine model", *Medical Physics* 32 (3), 733-743.

5. Ross AB, Diederich CJ, Nau WH, Gill H, Bouley DM, Daniel B, Rieke V, Butts RK and Sommer G (2004), "Highly directional transurethral ultrasound applicators with rotational control for MRI-guided prostatic thermal therapy", *Phys Med Biol*, 49:189-204.

6. Davidson, S.R.H., Vitkin, I.A., Sherar, M.D. & Whelan, W.M. "Characterization of measurement artefacts in fluoroptic temperature sensors: Implications for laser thermal therapy at 810 nm". *Lasers in Surgery and Medicine* 36, 297-306 (2005).

7. Hazle, J.D., Stafford, R.J. & Price, R.E. "Magnetic resonance imaging-guided focused ultrasound thermal therapy in experimental animal models: Correlation of ablation volumes with pathology in rabbit muscle and VX2 tumors". *Journal of Magnetic Resonance Imaging* 15, 185-194 (2002).

8. Chin, L.C.L., Wilson, B.C., Whelan, W.M. & Vitkin, I.A. "Radiance-based monitoring of the extent of tissue coagulation during laser interstitial thermal therapy". *Optics Letters* 29, 959-961 (2004).

9. Veltri, A., De Fazio, G., Malfitana, V., Isolato, G., Fontana, D., Tizzani, A., and Gandini, G. "Percutaneous US-guided RF thermal ablation for malignant renal tumors: Preliminary results in 13 patients". *European Radiology* 14, 2303-2310 (2004).

10. Ritz, J., Roggan, A., Isbert, C., Muller, G., Buhr, H. and Germer, C. "Optical properties of native and coagulated porcine liver tissue between 400 and 2400 nm". *Lasers in Surgery and Medicine*, 29, 205-211 (2001).

11. Soroushian, B, Whelan, W. and Kolios, M. "Assessment of opto-mechanical behavior of biological samples by interferometry". *Photons Plus Ultrasound: Imaging and Sensing*, SPIE (2009).